Simple lipids form stable higher-order structures in concentrated sulfuric acid

Daniel Duzdevich[1,2,†*], Collin Nisler[1,†], Janusz J. Petkowski[3,4,5], William Bains[3,6], Caroline K. Kaminsky[1], Jack W. Szostak[1,7], Sara Seager[3,8,9]

[1] Department of Chemistry, The University of Chicago, Searle Chemistry Laboratory, Chicago, IL 60637, USA
[2] Freiburg Institute for Advanced Studies, Albert-Ludwigs-Universität Freiburg, 79104 Freiburg im Breisgau, Germany
[3] Department of Earth, Atmospheric and Planetary Sciences, Massachusetts Institute of Technology, 77 Massachusetts Avenue, Cambridge, MA 02139, USA
[4] Faculty of Environmental Engineering, Wroclaw University of Science and Technology, 50-370 Wroclaw, Poland
[5] JJ Scientific, Mazowieckie, Warsaw, Poland
[6] School of Physics and Astronomy, Cardiff University, 4 The Parade, Cardiff CF24 3AA, UK
[7] Howard Hughes Medical Institute, The University of Chicago, Chicago, IL 60637, United States of America
[8] Department of Physics, Massachusetts Institute of Technology, 77 Massachusetts Avenue, Cambridge, MA 02139, USA
[9] Department of Aeronautics and Astronautics, Massachusetts Institute of Technology, 77 Massachusetts Avenue, Cambridge, MA 02139, USA

[†] Equal contribution
[*] To whom correspondence should be addressed. Email: dduzdevich@uchicago.edu

Running Title: lipids in sulfuric acid

Keywords: sulfuric acid, Venus, lipids, vesicles

Abstract

Venus has become a target of astrobiological interest because it is physically accessible to direct exploration, unlike exoplanets. So far this interest has been motivated not by the explicit expectation of finding life, but rather a desire to understand the limits of biology. The Venusian surface is sterilizing, but the cloud deck includes regions with temperatures and pressures conventionally considered compatible with life. However, the Venusian clouds are thought to consist of concentrated sulfuric acid. To determine if any fundamental features of life as we understand them here on Earth could in principle exist in these extreme solvent conditions, we have tested several simple lipids for resistance to solvolysis and their ability to form structures in concentrated sulfuric acid. We find that single-chain saturated lipids with sulfate, alcohol, trimethylamine, and phosphonate head groups are resistant to sulfuric acid degradation at room temperature. Furthermore, we find that they form stable higher-order structures typically associated with lipid membranes, micelles, and vesicles. Finally, results from molecular dynamics simulations suggest a molecular explanation for the observed robustness of the lipid structures formed in concentrated sulfuric acid. We conclude with implications for the study of Venus as a target of experimental astrobiology.

Introduction

The catalogue of confirmed exoplanets continues to grow (Christiansen, 2022), and the James Webb Space Telescope has improved our ability to measure the transmission spectra of exoplanet atmospheres (Gardner et al., 2006). However, characterizing the physical properties of exoplanets that are relevant to habitability remains extraordinarily challenging. Concurrently, astrobiologists have turned their attention to our solar system, especially Mars, Europa, Enceladus, and more recently Venus, as accessible to direct astrobiological exploration. An astrobiological perspective on the solar system seeks to compare what we know about Earth biology with what we are learning about non-Earth environments thorough experiment and space missions. Some of our solar system neighbors, like Venus, may appear at first glance to be completely uninhabitable, yet there is nonetheless active speculation about the potential habitability of Venus's sulfuric acid clouds (see for example (Bains et al., 2021a, 2023; Grinspoon

and Bullock, 2007; Kotsyurbenko et al., 2021, 2024; Limaye et al., 2018; Mogul et al., 2021a; Morowitz and Sagan, 1967; Patel et al., 2021; Schulze-Makuch and Irwin, 2006; Seager et al., 2021)). However, deciding whether a planet is habitable requires consideration of whether the conditions on that planet are consistent with the conditions required by life (regardless of whether life actually exists there). Earth life remains the basis for such planetary habitability assessment, but the extent to which specifics of Earth life can be considered universal are disputed.

Venus is a critical test case for such astrobiological studies because the clouds consist of liquid concentrated sulfuric acid, which is considered incompatible with life, and contain almost no water, which is considered essential for life (e.g. (Hallsworth et al., 2021)). Despite these challenges, speculation about life in the clouds of Venus persists because of anomalies in its atmospheric chemistry (e.g. (Bains et al., 2021b; Limaye et al., 2018; Mogul et al., 2021a, 2021b; Petkowski et al., 2024b)). A rigorous astrobiology research program, centered around organic chemistry, should consider the fundamental features of life as we know it-and seek to explore its limits with reference to known environments on other worlds, including Venus.

Organic chemistry in concentrated sulfuric acid is rarely studied yet surprisingly rich, with recent work supporting the notion that complex organic molecules, including amino acids and nucleobases, can be stable in this unusual solvent (Petkowski et al., 2024a; Seager et al., 2024a, 2023, 2024b; Spacek et al., 2024). These results build on isolated reports from decades ago that considered the chemical behavior of organic molecules in concentrated sulfuric acid long before its importance for planetary science was realized, or the sulfuric acid composition of the Venusian clouds was known (*e.g.*: (Albright et al., 1972; Habeeb, 1961; Miron and Lee, 1963; Reitz et al., 1946; Schumacher and Günther, 1983; Steigman and Shane, 1965; Wagner and von Philipsborn, 1971)).

The stability of simple organic molecules in concentrated sulfuric acid is an interesting observation, and without such stability no life could be possible, but life also requires more complex structures for biological function. One fundamental feature of life is cellularity: the differentiation of "inside" (the contents of a cell, including information, molecules, and all their interactions) and "outside" (the environment), in addition to a

mechanism for communication and exchange between the two. Cellularity also enables the distinction between encoded genotype (information internal to the cell) and expressed phenotype (the relationship of that information with the environment), a prerequisite for Darwinian evolution. Interpreting cellularity as a feature of life does not necessarily imply Earth biology (a DNA-encoded genotype, for example).

Biology uses lipid membranes to define cells. Unlike proteins and nucleic acids, biological lipids take on a broad range of chemistries. They must form effective membranes that can grow, divide in response to the cellular division machinery, and remain stable in the given cell's environment. The primary role of cell membrane lipids is to physically define the cell, demarcating inside from outside. The cell membrane is especially important in extreme environments because it must help maintain the homeostasis of the intracellular environment against otherwise harsh external conditions. Reasoning that with our current understanding of biology we cannot envision life without cells, we here consider whether simple lipids might be resistant to sulfuric acid, and further, whether they can form higher-order structures such as membranes and vesicles typically considered a prerequisite for life-like phenomena.

The formation of micelles or membranous structures in non-aqueous solvents has attracted little attention. We identified only eleven papers that report the behavior of surfactants and other amphiphilic molecules in concentrated sulfuric acid (McCulloch, 1946; Menger and Jerkunica, 1979; Müller, 1991b, 1991c, 1991a; Müller and Burchard, 1995; Müller and Giersberg, 1992, 1991; Müller and Miethchen, 1988; Steigman and Shane, 1965; Torn and Nathanson, 2002). Several of these studies report the formation of micelles and other lipid structures.

Our research has also been inspired by the extensive literature on the potential role of fatty acids in the emergence of life on Earth (*e.g.*: (Apel et al., 2002; Deamer, 2016; Gebicki and Hicks, 1973; Hargreaves and Deamer, 1978; Mansy, 2009)). These simple single-chain lipids can form vesicles made of canonical lipid bilayers if the pH of the aqueous solution is near the pK_a of the fatty acid carboxylic acid head groups (typically ~ pH 8 in the context of a membrane) (Kanicky and Shah, 2003). Under these conditions, approximately half of the headgroups will be deprotonated, and the other

half protonated, so that charge interaction networks among the headgroups stabilize the hydrophilic bilayer surfaces.

We identify several simple lipids that appear to have similar properties in the context of aqueous sulfuric acid solvent in concentrations up to 90% (v/v). We challenge the assumption that concentrated sulfuric acid is inherently incompatible with basic properties of the chemistry of life, and specifically show that complex solvent-enclosing lipid vesicles can form, are stable, and can dynamically re-arrange and form higher-order structures in concentrated sulfuric acid. While the extreme corrosiveness of sulfuric acid limits our experimental toolkit and ability to comprehensively characterize the biophysical properties of these structures, we posit that they are consistent with lipid bilayer membranes. Our data suggest that micelles, vesicles, oil droplets, and under some conditions extensive membrane networks may be forming. These results signal an opportunity to experimentally push the boundaries of prebiotic chemistry into a regime that is relevant for studying Venus from an astrobiological perspective.

Materials and Methods

General

Lipids were from Sigma-Aldrich (decyltrimethylamine, octadecyltrimethylammonium, decylphosphonate) or Combi-Blocks (octadecylsulfate, decylsulfate) at the highest available purity without further purification. Sulfuric acid was from Sigma-Aldrich (nominally 95-99%). Experimental sulfuric acid concentrations are reported as volume/volume (v/v) percentages (volume sulfuric acid / total volume sulfuric acid + water) unless otherwise noted. Water was from a Millipore Milli-Q filtration system with a polisher filtration attachment. Glass vials for sample preparation were from ChemGlass, with PTFE-backed caps. All glassware was rinsed with sulfuric acid solvent prior to experimental use. Deuterated NMR reagents and internal standards were from Sigma-Aldrich or Cambridge Isotope Laboratories.

NMR spectroscopy

Samples were prepared by measuring out the appropriate mass of dry lipid in a 4 ml glass vial and adding the previously-prepared aqueous sulfuric acid. The vial was sealed with a PTFE-lined cap and the mixture gently inverted by hand and allowed to incubate at room temperature for at least one hour. For extractions, the $CDCl_3$ was added directly to the vial, the mixture inverted gently by hand, and the phases allowed to separate over several minutes. The solution was transferred to pre-rinsed NMR vials with a pre-rinsed glass pasteur pipette. NMR spectra were acquired on a Varian INOVA NMR spectrometer operating at 400 MHz for ^1H spectra and 161 MHz for ^{31}P spectra. Measurements were locked to D_2O or $CDCl_3$. Chemical shifts (δ) are shown in parts per million (ppm). Spectra were processed and analyzed with MestReNova v14.2.0 (Mestrelab Research) (Willcott, 2009).

DLS measurements
Samples were prepared by measuring the appropriate mass of dry lipid in a 4 ml glass vial and adding 2 ml of 70%, 80%, or 90% aqueous sulfuric acid. Samples were placed on a rocker for ~ 2 hours at 20 rpm, after which they were transferred to a glass cuvette with a PTFE cap (Malvern PCS1115) and the day 0 measurements were taken. For the first set of experiments, readings were taken after 24 hours and after 5 days. For subsequent analysis of the 50/50 mix of decylsulfate and decyltrimethylamine C10 (SDS, DTMA) or octadecylsulfate and octadecyltrimethylammonium C18 (SOS, TMO) lipids, measurements were taken hours after preparation, after 24 hours, 3 days, and 7 days, unless otherwise indicated. After each measurement, the sample was immediately returned to the rocker. Before each use, vials and cuvettes were cleaned by rinsing in Milli-Q water, detergent, another rinse of Milli-Q water, then acetone under vacuum. Measurements were acquired on a Zetasizer Nano ZS at a backscatter detection angle of 175° at 25°C. 3 measurements were taken in 3 runs each for 60 seconds in the first set of experiments, and for the 50/50 mix of decylsulfate and decyltrimethylamine measurements were taken in 3 runs for 1000 seconds per run. The viscosity and refractive index for the indicated sulfuric acid concentrations were taken from the literature (Beyer et al., 1996; Liler, 1971; Rhodes and Barbour, 1923) and used as dispersant parameters in the respective measurements, and attenuator position was

determined automatically. Particle sizes were taken from the resultant intensity distribution.

Confocal microscopy

For visualization of samples prepared identically as in DLS experiments, 2 µl of sample was placed in the center of a µ-Slide 18-well sterilized, uncoated glass bottom plate (Ibidi). For subsequent confocal experiments, vesicles were first prepared in water by measuring the appropriate amount of lipid for a final concentration of 75 mM in a 4 ml glass vial and adding 2 ml of water. After vortexing for ~5 seconds, 75 mM KOH was added, and the sample was again vortexed. Aliquots of this sample were added to a µ-Slide 18 well glass bottom plate (Ibidi) to 5 wells, and sulfuric acid was added for a 10%, 50%, 70%, 80%, or 90% final concentration of sulfuric acid. For imaging of samples between glass slides, slides were placed in 1 M NaOH for 5 minutes, 1 M HCl for 5 minutes, then washed with deionized water. 2 µl total (lipids plus sulfuric acid) was placed in the center of an imaging spacer (VWR) between slides. For all samples, BODIPY (Sigma) was added in a final concentration of 2.5 µM. Samples were excited at 568 nm and imaged by confocal microscopy on an A1R/Ti setup (Nikon) using a 1.45 NA 100× CFI Plan Apochromat objective.

Molecular Dynamics Simulations

100 × 100 Å membrane patches of the pure decylsulfate (Sys1), pure decyltrimethylamine (Sys2), and a 50/50 mix of decylsulfate and decyltrimethylamine (Sys3) were generated by the CHARMM-GUI (Jo et al., 2008) membrane builder. TIP3P waters were added 25 Å above and below the bilayer using the autosolvate plugin in Visual Molecular Dynamcis (VMD) (Humphrey et al., 1996). In house Tcl scripts were used to replace all water molecules with sulfuric acid and hydronium ions such that the final concentration of sulfuric acid was 70% with a net zero charge. Two water molecules were removed for every sulfuric acid added, and one water molecule was removed for each hydronium ion added. The ratio of protonated and deprotonated sulfuric acid molecules was adjusted for each system to result in a net zero charge. The standard CHARMM36 (Huang and Mackerell, 2013; Vanommeslaeghe and MacKerell,

2012) forcefield was used for the lipids and sulfuric acid, while parameters for the hydronium ions were taken from previously published results (Sagnella and Voth, 1996). The NAMD 2.14 (Melo et al., 2018; Phillips et al., 2020) program was used to perform all classical and hybrid quantum mechanical/molecular mechanic (QM/MM) simulations, while ORCA (Neese et al., 2020) was used to perform quantum calculations. Analysis was performed and images were generated using VMD.

To prepare for QM/MM simulations, all systems were minimized for 1000 steps and equilibrated in the *NpT* ensemble at 1 atm using a hybrid Nosé-Hoover Langevin piston method, and temperature was controlled using Langevin dynamics with a damping coefficient of $\gamma = 1$. Nonbonded interactions were switched off at 12 Å and long-rang interactions were calculated using the Particle-Mesh Ewald method. Bonds involving hydrogen atoms were fixed using the SHAKE algorithm. At the end of the equilibration, quantum regions were selected to include three interacting lipids: two decylsulfate and one decyltrimethylamine in Sys3, one sulfuric acid molecule and five hydronium molecules for Sys1, two sulfuric acid molecules and one hydronium molecule for Sys2, and three hydronium ions and one sulfuric acid molecule for Sys3 (Figure 5 A). Two such regions were selected for each system, resulting in six total QM/MM simulations (Sys1a-b, Sys2a-b, and Sys3a-b). The hydronium ions, the sulfuric acid molecule, and the head groups of all lipids to the C1 carbon atom of the lipid tail were all treated at the QM level (49 atoms total for Sys1a-b, 62 atoms total for Sys2a-b, and 49 atoms total for Sys3a-b) resulting in a multiplicity of 1 and a net zero charge for all systems. The HF-3c semi-empirical Hartree Fock method was used to simulate the QM region (Sure and Grimme, 2013), chosen due to its ability to describe large biomolecular systems to an accuracy that approaches large-basis methods at a fraction of the computational cost. Interactions between the QM and MM region were treated with an electrostatic embedding scheme, and covalent bonds split at the QM/MM boundary were treated with a Charge Shifting method. Charge distribution in the QM region was taken from ORCA and updated at every step. A 0.5 fs timestep was used, and remaining parameters for the classical region were identical to those used for the equilibration. Self-consistent field electron density and electrostatic potential maps were

generated using the orca_plot command and the molecular orbitals output by ORCA, and plotted with an isovalue of 0.09.

Results

Lipid selection

We began by selecting a set of simple lipids that are commercially available at high purity, with saturated hydrophobic tails, and without acid-labile ethers and esters. We limited the tail lengths to 10 or 18, a regime that should be generally soluble but still hydrophobic enough to promote bilayer formation. Finally, we sought to include head groups that could in principle form charge-charge interactions, analogous to what is observed with biological lipids, even under heavily protonating conditions. Here we chose to work with trimethylamine, sulfate, and phosphonate head groups (Caschera et al., 2011; Liu et al., 2018; Walde et al., 1997). We note that other lipids and combinations could be considered in the future.

NMR spectra show that the lipids are resistant to sulfuric acid solvolysis at room temperature

We used NMR to test the resistance of each C10 lipid to attack by sulfuric acid at room temperature. At 100 mM, all the selected lipids are poorly soluble in water and concentrated sulfuric acid. However, at 50 mM, decyltrimethylamine is soluble in both water and concentrated sulfuric acid (Figure 1). We incubated 50 mM decyltrimethylamine ($C_{13}H_{30}N^+$) with D_2O, D_2O + 1% H_2SO_4, or 30% D_2O + 70 % D_2SO_4 for at least one hour before acquiring an ^1H spectrum. 1% (v/v) aqueous H_2SO_4 corresponds to a measured pH $\cong$ 0.8. We observed no additional peaks or changes to the peaks identified in water under the acidic conditions. Further, the proton ratios remained stable across all conditions. We conclude that decyltrimethylamine is resistant to sulfuric acid in concentrations up to 70%.
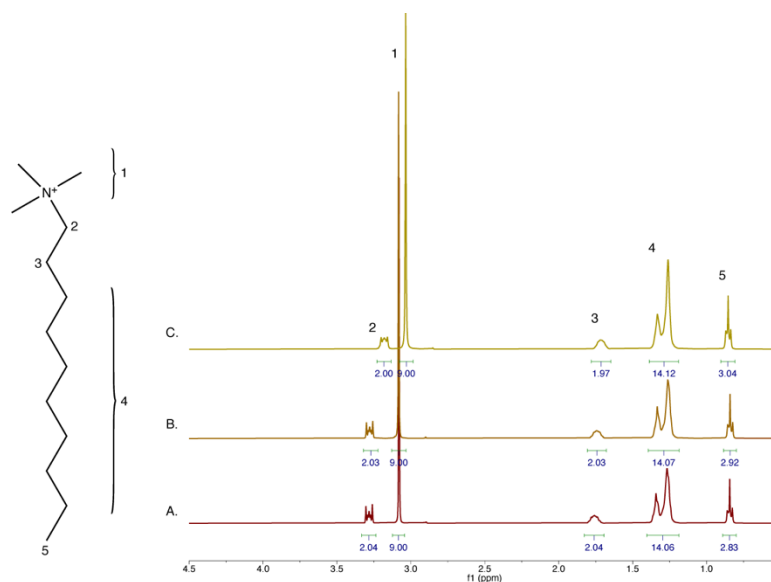
Figure 1. Decyltrimethylamine is resistant to 70% (v/v) sulfuric acid. ^{1}H NMR spectra of 50 mM decyltrimethylamine in (A) D_2O, (B) D_2O + 1% H_2SO_4, and (C) 30% D_2O + 70% D_2SO_4. The measured proton ratios are in excellent agreement with the expected ratios and do not change with increasing sulfuric acid concentration. Note the absence of new peaks. Spectra were referenced to DSS at 0 ppm, and the integrals normalized to the 9 protons assigned to peak 1.
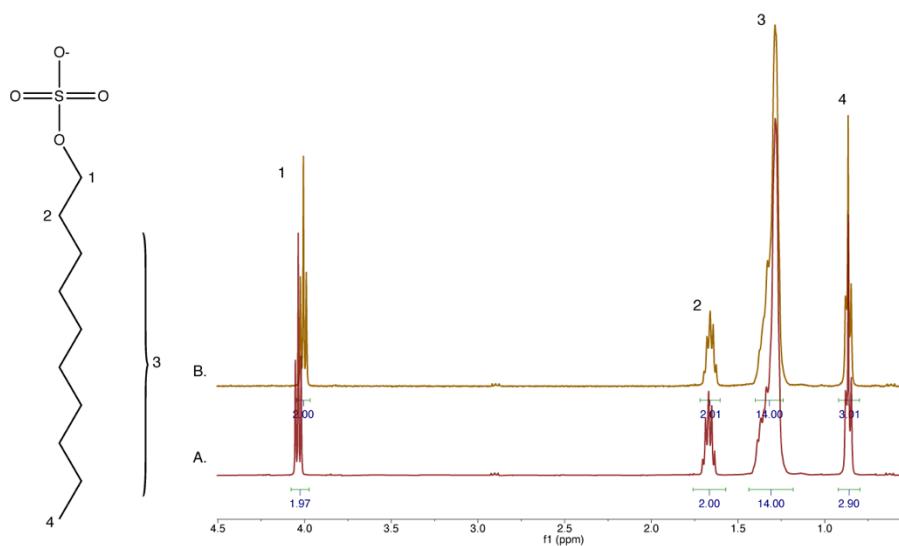

Figure 2. Decylsulfate is resistant to low-concentration sulfuric acid. ^{1}H NMR spectra of 50 mM decylsulfate in (A) D_2O, and (B) D_2O + 1% (v/v) H_2SO_4. The measured proton ratios are in excellent agreement with the expected ratios and do not change with added sulfuric acid. Note the absence of new peaks. Spectra were referenced to DSS at 0 ppm, and the integrals normalized to the 14 protons assigned to peak 3.

Decylsulfate ($C_{10}H_{22}O_4S$) is resistant to 1% H_2SO_4 (Figure 2). However, at 50 mM it is poorly soluble in 70% sulfuric acid and yields low-quality NMR data. Therefore,

we incubated decylsulfate in 70% H$_2$SO$_4$ for one hour and extracted the mixture into CDCl$_3$ for NMR analysis (Figure 3). Several new peaks appeared after 70% acid treatment (compare Figure 2A to Figure 3A) which we hypothesized arise from decyl alcohol. A spike-in of authentic standard confirmed the assignment (Figure 3B). We conclude that after 1 hour in 70% sulfuric acid, approximately 20% of the sulfate headgroups are in the alcohol form. This is probably due to acid-catalyzed hydrolysis of protonated sulfate. Decyl alcohol can participate in lipid bilayer formation in the context of other lipids.

Decylphosphonate is too poorly soluble in both water and 70% sulfuric acid to generate quality NMR spectra, so we applied the CDCl$_3$ extraction approach for all conditions (Figure 4). We find decylphosphonate is stable in up to 70% sulfuric acid, and note the presence of fully protonated phosphonate at the highest tested acid concentration (Supplemental Figure 1).

We conclude that sulfuric acid in concentrations up to 70% does not affect decyltrimethylamine, protonates the sulfate head group in decylsulfate and catalyzes the formation of ~20% decyl alcohol, and protonates the phosphonate of decylphosphonate. With the exception of the ~20% decyl alcohol, we observed no acid-catalyzed degradation of any bonds in any of these compounds at room temperature over the duration of the experiments.
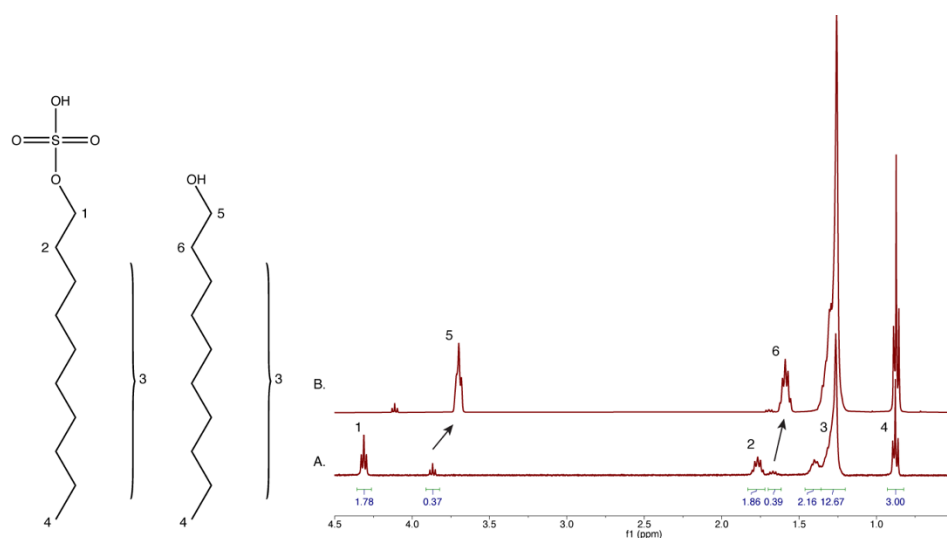

Figure 3. Decylsulfate is largely resistant to 70% (v/v) sulfuric acid. ^{1}H NMR spectra of (A) 50 mM decylsulfate incubated in 30% D$_2$O + 70% H$_2$SO$_4$ for 1 hour and extracted into CDCl$_3$, and (B) spike-in of

decyl alcohol. Compare with Figure 2. We assign the extra peaks upfield of 1 and 2 to the alcohol-adjacent hydrogens in the context of the alcohol, as confirmed by the spike-in of a decyl alcohol standard (B). The peak integral ratios suggest that approximately 20% of the lipids are in the alcohol form upon exposure to concentrated sulfuric acid. Spectra were referenced to TMS at 0 ppm, and the integrals normalized to the 3 protons assigned to peak 4.
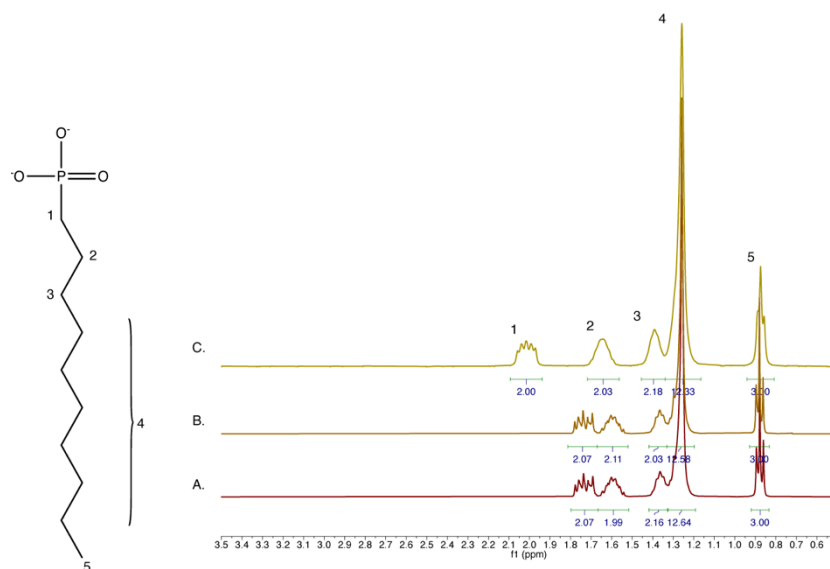

Figure 4. Decylphosphonic acid is resistant to 70% (v/v) sulfuric acid. ^{1}H NMR spectra of 50 mM decylphosphonic acid incubated in (A) D_2O, (B) D_2O + 1% H_2SO_4, and (C) 30% D_2O + 70% H_2SO_4 for one hour and extracted into $CDCl_3$. The measured proton ratios are in good agreement with the expected ratios and do not change with increasing sulfuric acid concentration. Note the absence of new peaks. Peaks 1 and 2 shift downfield as the phosphonate is protonated (see Supplemental Figure 1). Spectra were referenced to TMS at 0 ppm, and the integrals normalized to the 3 protons assigned to peak 5.

Dynamic Light Scattering shows the formation of higher-order lipid structures in concentrated sulfuric acid

To determine if trimethylamine, phosphonate, and sulfate lipids form any higher-order structures in concentrated sulfuric acid, dynamic light scattering (DLS) was employed to obtain the size distribution of lipid aggregates in solution. Initial measurements of 25 mM decylphosphonate, decyltrimethylamine, decylsulfate, an equimolar mix of all 3 lipids, and a 50/50 equimolar mix of decylphosphonate and decyltrimethylamine were taken in 70% sulfuric acid 24 hours after preparing samples and 5 days after preparing samples. Intensity peaks were observed between 100 and 1000 nm for all 4 samples,

indicating the presence of higher-order structures larger than micelles, regardless of the identity of the lipid head group (Supplemental Figure 2).[1] In addition, signals were observed above 1000 nm for all samples, suggesting the presence of larger structures. While dust particles or other contaminants could potentially contribute to signals above 1000 nm, microscopy results (see below) show lipid aggregates at this scale, suggesting that these signals are likely not due to contaminants.

Decylphosphonate exhibited significantly larger aggregate sizes at both day 2 and day 5 compared to all other samples except for the mix of all 3 lipids at day 2, suggesting that the identity of the headgroup has an effect on the biophysical properties of the lipid structures in sulfuric acid solution. The mix of decylsulfate and decyltrimethylamine exhibited the most stable and least variable signal between measurements, and between day 2 and day 5, so lipids with these head groups were selected for further analysis.
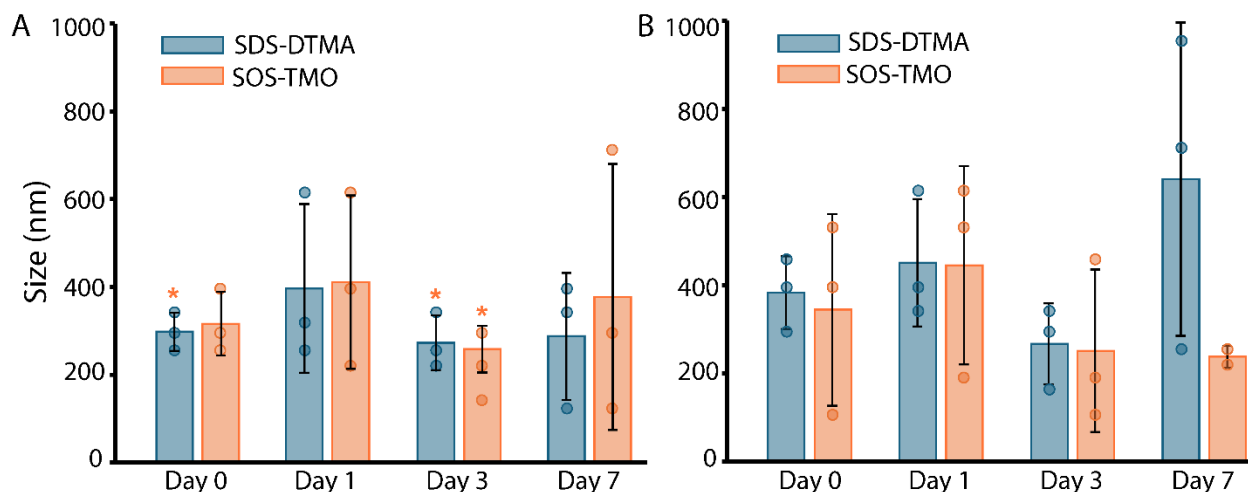

Figure 5. Lipids form stable structures in concentrated sulfuric acid. DLS readings of 75 mM decylsulfate and decyltrimethylamine (SDS-DTMA, blue) and 1 mM octadecylsulfate and octadecyltrimethylammonium (SOS-TMO, orange) lipids prepared in 70% sulfuric acid (A) and 80% sulfuric acid (B). Average values of independent replicates for each lipid preparation are shown by the solid bar, individual values are indicated by circles, and standard deviations are shown in black. Orange asterisks indicate samples that exhibit a significantly different average to that of the day 5 25 mM SDS-

---

[1] Note that the sizes of micelles and vesicles are determined by the physical properties of the lipids. Simple single-chain lipids form micelles of ~5-20 nm, and vesicles of ~100-1000 nm in aqueous solution. The size distributions of micelles and vesicles observed in concentrated sulfuric acid are similar to those observed for fatty acids in water.

DTMA measurements (Supplemental Figure 2F). These results show that SDS-DTMA and SOS-TMO lipids form structures in 70% and 80% sulfuric acid on the same scale as fatty acid vesicles.

To better characterize the changes in size distribution over time and at higher concentrations of sulfuric acid, we prepared a 50/50 equimolar mix of 75 mM C10 decylsulfate and decyltrimethylamine (SDS-DTMA) in 70%, 80%, and 90% sulfuric acid. Furthermore, to determine the effect of chain length on the size distribution of these lipids, a 50/50 equimolar mix of 1 mM C18 octadecylsulfate and octadecyltrimethylammonium (SOS-TMO) was also tested in 70%, 80%, and 90% sulfuric acid. DLS readings were taken a few hours after preparation (day 0), and again after 1, 3, and 7 days. 3 independent replicates were prepared and measured identically for all samples (Figure 5; Supplemental Figure 3). Signals between 100 and 1000 nm, which will roughly correspond to the size of lipid vesicles, were recorded at the peak intensity value. SDS-DTMA but not SOS-TMO changed color in 80% and 90% sulfuric acid over the course of the seven days, becoming increasingly dark and ultimately almost black (Supplemental Figure 4). Despite this change in coloration of the solution, the average sizes of lipid structures were not significantly different between chain lengths or over the seven day incubation. In addition, with 3 exceptions (SDS-DTMA in 70% sulfuric acid at day 0 and day 3, SOS-TMO in 70% sulfuric acid at day 3; Figure 5A, orange asterisks), the average sizes of SDS-DTMA and SOS-TMO lipid aggregates in 70% or 80% sulfuric acid were not significantly different than the initial 25 mM SDS-DTMA readings (Supplemental Figure 2E). However, at 90% sulfuric acid, only SDS-DTMA and SOS-TMO at day 0, and SOS-TMO at day 7 exhibited peaks between 100

and 1000 nm on more than one repeat (Supplemental Figure 5), suggesting that at higher concentrations of sulfuric acid these structures become more heterogeneous or destabilized. The high viscosity of sulfuric acid may also contribute to the size of vesicle-like structures. Together, the DLS results suggest that the size distribution of
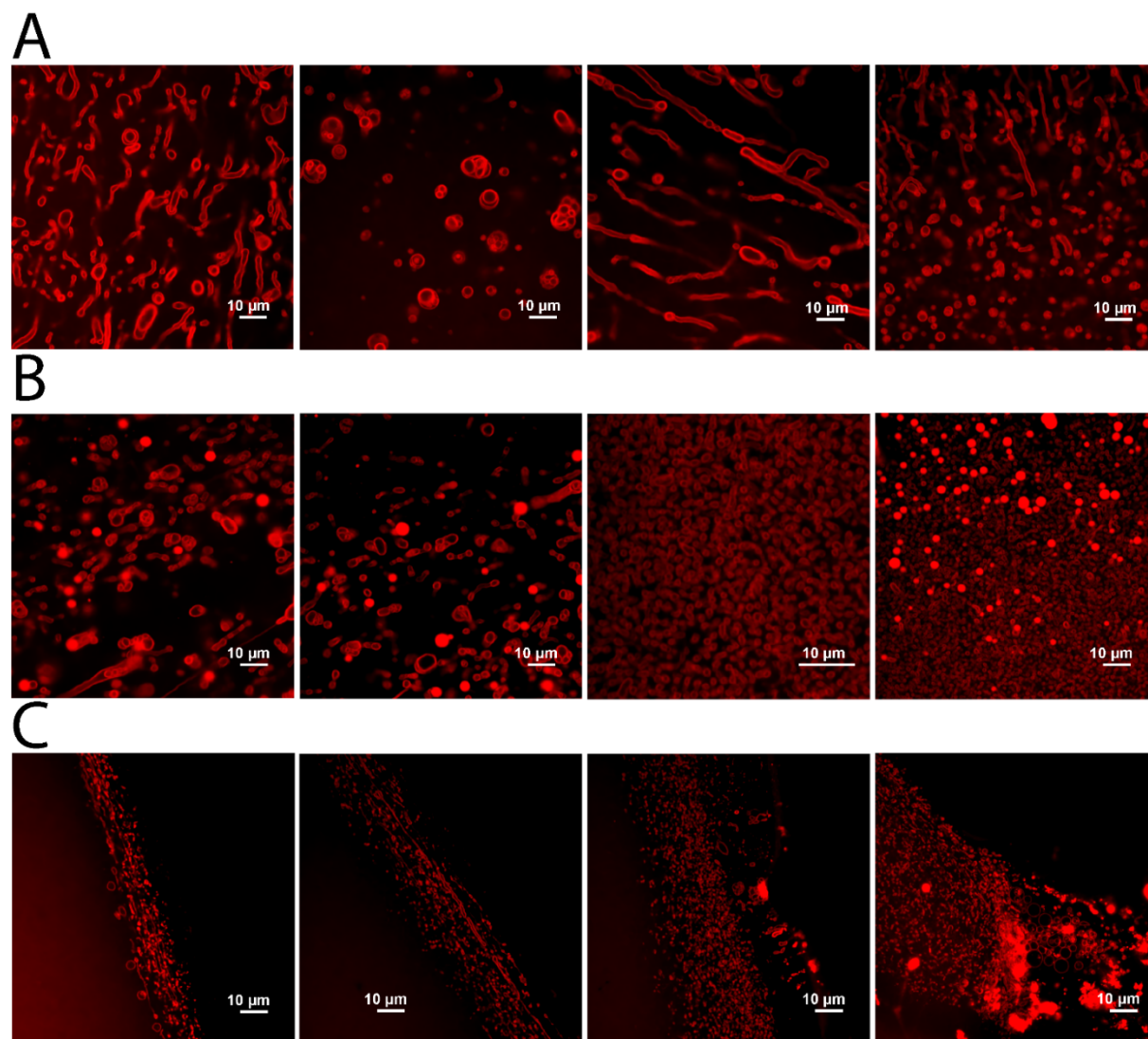

Figure 6. Vesicle-like structures form after addition of concentrated sulfuric acid to solid lipids. Confocal images of BODIPY stained SDS-DTMA lipids from samples prepared in 70% (A), 80% (B), and 90% (C) sulfuric acid. In all samples, vesicles of varying size and other lipid structure morphologies are observed. Each panel is a different region of the same sample, taken on the same day. These results indicate that the signals observed in the DLS readings are due to the presence of lipid-based structures.

lipid structures in concentrated sulfuric acid below 90% are largely unaffected by lipid concentration or chain length and remain stable on the timescale of days.

Confocal microscopy confirms the formation of higher-order lipid structures in concentrated sulfuric acid

Our DLS measurements suggest that structured lipid aggregates can form in concentrated sulfuric acid. To determine the morphology of these structures, we used confocal microscopy to visualize 4,4-difluoro-4-bora-3a,4a-diaza-*s*-indacene (BODIPY) stained lipids. Samples were prepared identically as in the DLS experiments and placed in the center of an 18-well uncoated, sterilized glass bottom slide such that samples did not contact the walls of the chamber. 2.5 µm BODIPY was then added to each sample. Surprisingly, the organic BODIPY dye showed robust fluorescence despite the concentrated sulfuric acid solvent. In all samples, vesicle-like structures of various sizes and lipid morphology were observed (Figure 6), corresponding to the range of sizes observed in the DLS signals. The presence of these structures is strictly dependent on the addition of lipids, eliminating the possibility that the observations are an artifact of sulfuric acid interaction with the slide surface. In 70% and 80% sulfuric acid, vesicle-like structures were distributed throughout the sample, while in 90% sulfuric acid, they were segregated to the periphery of the sample. This suggests a possible gradient in sulfuric acid concentration within the sample with vesicles only able to form in a local region of lower acid concentration. This may be an artifact of the hygroscopic sulfuric acid absorbing moisture from the air. These results suggest that SDS-DTMA lipids can form membranous, vesicle-like structures at sulfuric acid concentrations up to 90%. Additionally, all samples exhibited aggregates of widely varying sizes up to several microns, which agrees with the polydisperse samples suggested by the DLS readings (Figure 5; Supplemental Figure 2).
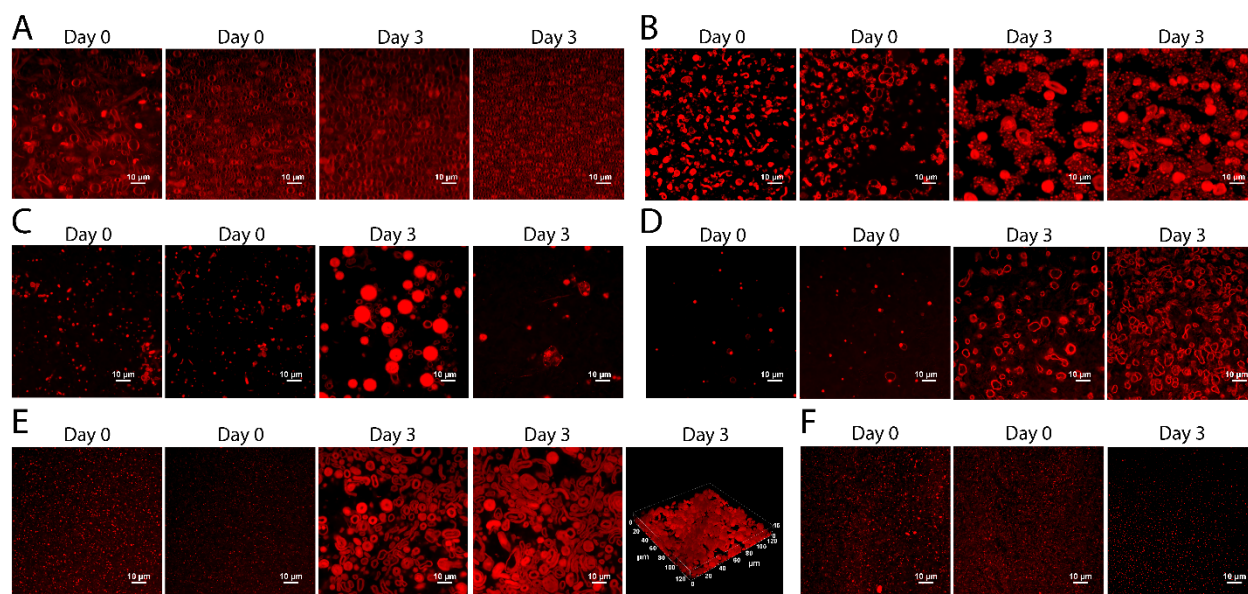
Figure 7. Vesicles formed in water persist after addition of sulfuric acid. Confocal images of BODIPY stained SDS-DTMA lipids at day 0 and day 3 at (A) 0%, (B) 10%, (C) 50%, (D) 70%, (E) 80%, and (F) 90% sulfuric acid. The final frame of (E) is a 3-dimensional *z*-stack image of that shown in the fourth panel. These results show that pre-formed vesicles persist after the addition of concentrated sulfuric acid.

Next we tested the ability of pre-formed SDS-DTMA vesicles in water to resist destabilization upon exposure to sulfuric acid. Lipids were prepared in water, and aliquots from this initial sample were added to individual glass bottom wells. Sulfuric acid was added to each well for a final concentration of 10%, 50%, 70%, 80%, or 90%, and BODIPY was added to a final concentration of 2.5 μm. Images were taken shortly after preparing samples, and 3 days after sample preparation (Figure 7). In the sample without sulfuric acid, multilamellar structures were abundant (Figure 7A), and adopted a relatively consistent size, indicating that the SDS-DTMA mix readily forms vesicle-like structures in an aqueous environment. In the presence of 10% or 50% sulfuric acid, a change in morphology is observed relative to the 0% sample (Figure 7B-C). These samples exhibited a more heterogeneous composition, with the presence of generally thicker membranes and a more irregular spatial distribution of aggregates and non-membranous droplets. Vesicle-like structures are present in both 10% and 50% sulfuric acid at day 0 and day 3. A further change in morphology is observed in 70% and 80% sulfuric acid (Figure 7 D-E). At day 0, mostly aggregates or droplets are observed, but between day 0 and day 3 these droplets coalesce to form a series of multilamellar structures, resembling vesicles, with an apparent internal volume. A 3-dimensional

image of these structures shows that they adopt a distinct ovoid shape (Figure 7 E, final panel). Finally, at 90% sulfuric acid, no membranous structures were observed at day 0 or day 3 (Figure 7 F). These results suggest that vesicles formed by SDS-DTMA lipids remain stable when exposed to the addition of sulfuric acid below 90%.

In all samples besides those in 0% or 90% sulfuric acid, a significant change in membrane morphology was observed between day 0 and day 3 (Figure 7). This change could be the result of a structural rearrangement of lipids within the membrane due to the change in solvent properties, the heat released upon the addition of sulfuric acid, or osmotic shock upon addition of sulfuric acid. To determine if heat can induce a morphology change, 75 mM SDS-DTMA vesicles prepared as above were subjected to a heat shock of 65° C for 1 hour. While some change may have occurred (Supplemental Figure 6 A), the size and morphology appeared similar to that without heat shock (Figure 7 A). Additionally, adding water in the same volume and ratio to samples prepared in 70%, 80%, and 90% sulfuric acid did not result in the morphological change observed upon addition of the same volume of sulfuric acid (Figure 7). These results indicate that the changes observed between day 0 and day 3 in the presence of sulfuric acid are likely due to changes in lipid-solvent interactions, not the heat released upon addition of sulfuric acid or osmotic shock.
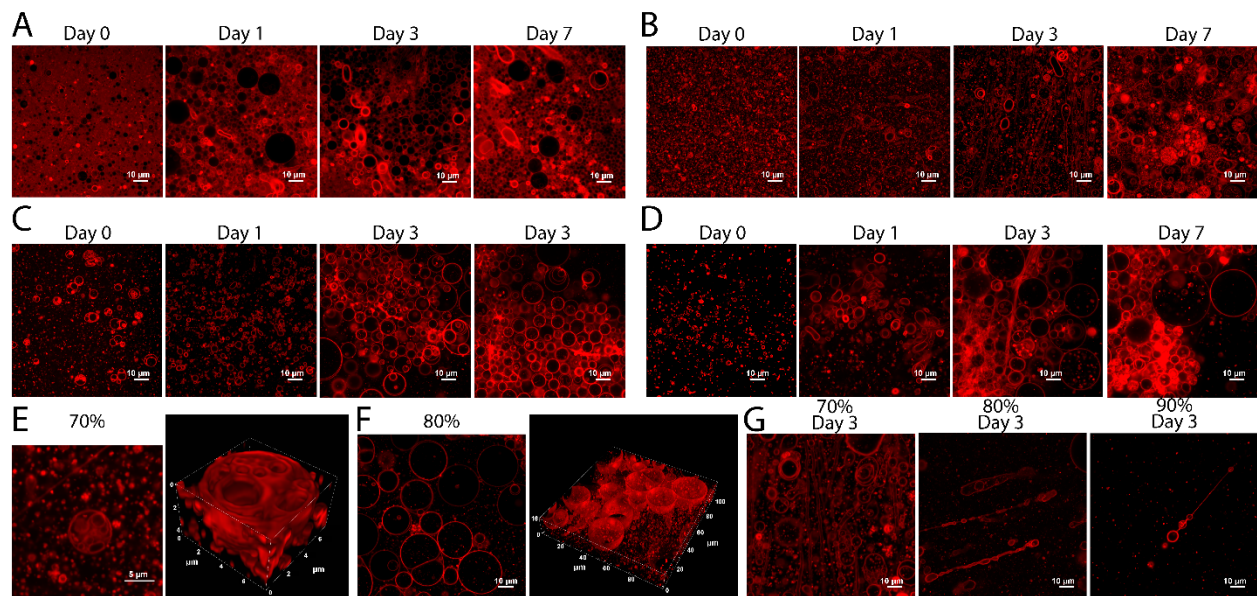

Figure 8. Vesicle-like structures persist in sulfuric acid over the course of 7 days. Confocal images of BODIPY stained SDS-DTMA lipids at day 0, day 1, day 3, and day 7 at (A) 0%, (B) 70%, (C) 80%, (D) 90% sulfuric acid. *z*-stack images showing the structure and internal volume of vesicle-like structures in (E) 70% and (F) 80% sulfuric acid. (G) Pearling and elongation of membranes was widespread in all

samples, and is shown for 70, 80, and 90% sulfuric acid. These images show that morphologically diverse vesicle-like structures are stable in sulfuric acid over the course of 7 days.

To ensure the structures observed in Figure 7 are not the result of interaction between sulfuric acid and the walls of the sample well, and to better characterize the temporal determinant of the observed morphology changes, we prepared SDS-DTMA samples in 70%, 80%, and 90% sulfuric acid as above but placed between glass slides such that sulfuric acid only contacted clean glass. Images were taken at day 0, day 1, day 3, and day 7 (Figure 8 A-D). All samples exhibited membranous vesicle-like structures of various sizes and morphologies with internal volumes (Figure 8 E-F). As in Figure 7, a change in morphology was observed after day 0 for all 3 samples. For all 3 samples with sulfuric acid, but not in the aqueous sample, a large, dense, and 3-dimensional cluster of vesicle-like structures with diverse sizes and lamellarity was observed at day 3 or day 7 (Figure 8 B-D, final frame). This clustering of vesicles may indicate a local exclusion of sulfuric acid in the interior of the cluster that has the effect of protecting the vesicles from disruption to their membranes. The mechanism behind the clustering could be positive surface charges bridged by sulfate anions, but further analysis will be required to explore this possibility. However, vesicles were found outside of the large cluster structures in all samples, both adhered to the surface and free-floating, indicating that while clustering between vesicles may provide some degree of protection, vesicles can exist individually in concentrated sulfuric acid. Additionally, elongation of the membrane up to tens of microns in length was seen in all 3 sulfuric acid samples but not in aqueous solvent (Figure 8G), often with associated pearling along the elongated segment. This behavior has been observed upon growth and mechanical perturbation of oleic acid vesicles in aqueous solvent and was proposed as a mechanism for vesicle growth and division (Zhu and Szostak, 2009). These results suggest that a similar cycle can be achieved in concentrated sulfuric acid with SDS-DTMA vesicles.
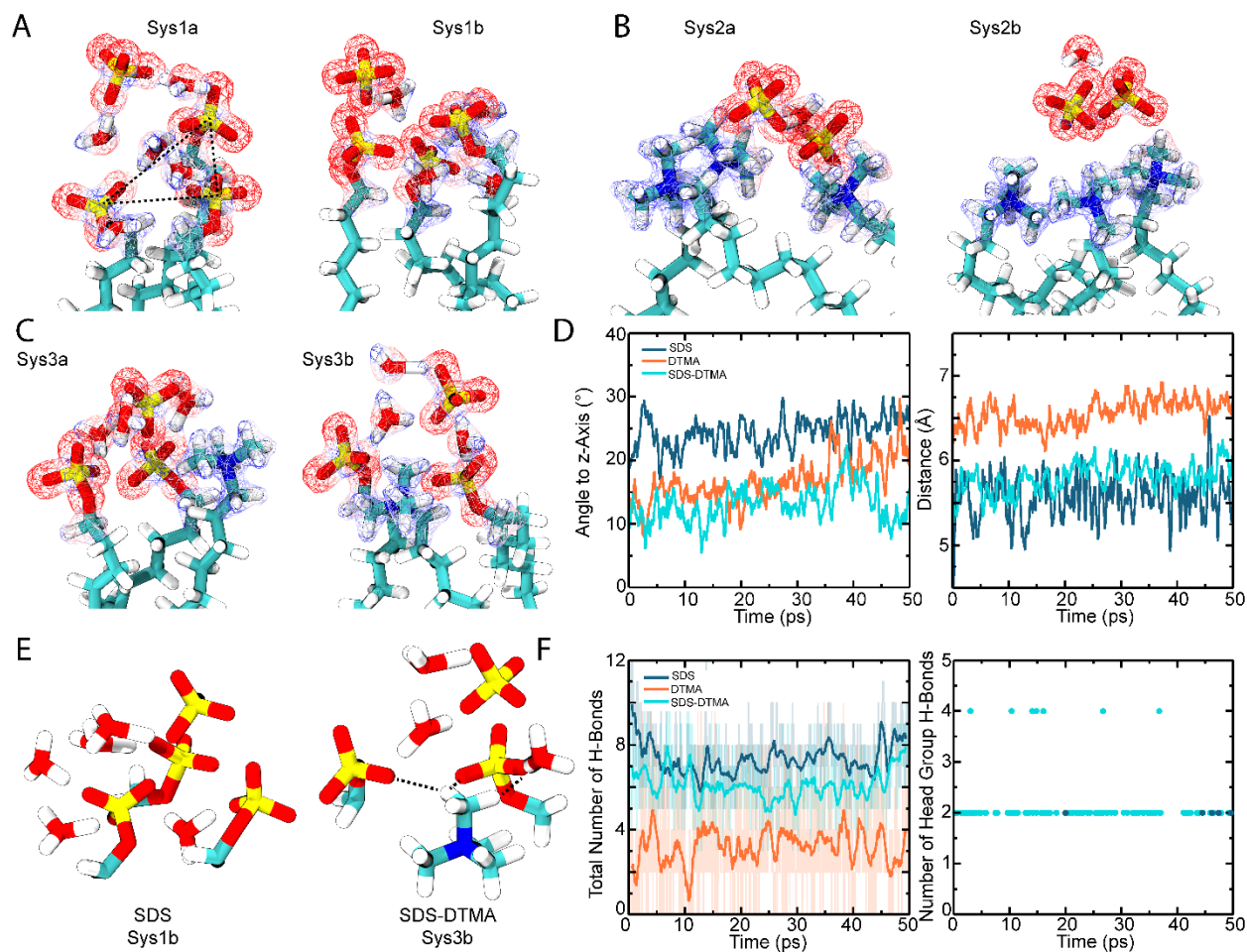
Figure 9. Modeling and Simulation of SDS and DTMA membranes. The final frame of the QM/MM simulations showing the electron density for the SDS only (A), DTMA only (B), and SDS-DTMA (C) systems. For clarity, only the lipids and solvent molecules associated with the QM region are shown. Dashed lines in (A) show the distances between head groups and the plane formed by the three head groups. (D) The angle between the axis perpendicular to the plane formed by the three head groups (left panel), and the average distances between head groups (right panel) are shown for all systems over the 50 ps simulations. (E) Snapshot of the SDS only system (left) and SDS-DTMA system (right), showing detail of the interaction between solvent molecules and head groups. Dashed lines indicate hydrogen bonds between head groups. (F) Total number of hydrogen bonds between all molecules (left panel; 0.6 ps running average shown in dark lines) and hydrogen bonds between head groups (right panel). The results of these simulations provide a potential mechanistic explanation for the robustness of SDS-DTMA membranes in sulfuric acid.

QM/MM modeling of the lipid bilayer membrane in concentrated sulfuric acid

Results of the confocal imaging suggest that SDS-DTMA membranes remain stable in the presence of sulfuric acid. To determine how the head groups of these lipids interact with each other and with concentrated sulfuric acid to maintain a stable membrane, two independent QM/MM simulations were run for 50 ps on a membrane patch composed of DTMA, SDS, or a 50/50 mix of SDS-DTMA lipids for a total of six simulations

(Supplemental Figure 7). For each system, three lipid head groups and interacting solvent molecules were treated at the QM level. At the end of each simulation, electron density and charge distribution was calculated. As expected, SDS head groups exhibited strong negative charge and DTMA head groups strong positive charge (Figure 9 A-C), resulting in a repulsion between like head groups and an attraction between oppositely charged head groups. The attractive forces result in a more energetically stable system with SDS-DTMA. Because the bilayer surface is perpendicular to the *z*-axis, deviation of the plane formed by the three lipid heads from the *x-y* plane can indicate the propensity for membrane deformations to form, making it more susceptible to solvent penetration. The angle between an axis perpendicular to the plane formed by the three lipid heads and the *z*-axis was tracked during all simulations, and the SDS-DTMA system exhibited the lowest angle on average (Figure 9 D, left panel). This indicates that the mixed lipid system remained most planar among all three systems.

Next, average distance between the center of mass of head groups was monitored during simulations. The SDS and SDS-DTMA systems exhibited the lowest average distances between head groups (Figure 9 D, right panel). These results suggest that, based on the dynamics of the lipid groups and their interactions, the stronger interactions in the mixed SDS-DTMA system make the bilayer more resistant to disruption by sulfuric acid. This disruption likely comes from perforation by sulfuric acid and hydronium ions, disrupting membrane continuity. In addition to inter-lipid interactions, interactions between lipids and solvent also suggest a mechanism by which a mix of DTMA and SDS lipids are more robust to destabilization by sulfuric acid. In the SDS-only systems, interactions between lipids were not direct, but facilitated by hydronium ions (Figure 9 A; Figure 9 E, left). This in turn leads to the penetration of hydronium molecules into the bilayer, which was not observed in the DTMA-only or SDS-DTMA systems (Figure 9 B-C). Furthermore, while the total number of hydrogen bonds was comparable between the DTMA-only and SDS-DTMA systems (Figure 9 E; F, left panel), almost none of the hydrogen bonds in the DTMA-only system come from interaction between head groups throughout the simulation (Figure 9 E; F, right panel). In the SDS-DTMA system, there is a robust network of hydrogen bonds between both the solvent and head groups and between head groups themselves, preventing solvent

molecules from penetrating beyond the head groups (Figure 9 E). Very few hydrogen bonds, either inter-lipid or lipid-solvent, were observed in the DTMA-only system (Figure 9 F). Collectively, the simulation results suggest the SDS-DTMA system forms stronger inter-lipid interactions and a more extensive hydrogen bonding network between lipids and solvent facilitated by a more even charge distribution across lipids, resulting in a more stable bilayer.

Discussion

Stable membranes that can form vesicles are likely to be an essential requirement for cellular life, no matter its chemical makeup. Water is highly favoured as a medium for life because in addition to being an excellent solvent for polar molecules and salts, many molecules are insoluble in water, allowing for the hydrophobic effect which drives the formation and the stability of membranes (Pohorille and Pratt, 2012; Pratt and Pohorille, 1992; Tanford, 1978). However, the ability to facilitate the formation of membrane structures is not a unique property of water. For example, ammonia (Griffin et al., 2015) and hydrogen fluoride (Roth et al., 1995) also have the dense hydrogen bonding networks required to drive a solvophobic effect in the liquid state (reviewed in (Bains et al., 2024)). Here we show the unexpected stability of complex membranous structures in another polar solvent: concentrated sulfuric acid.

Concentrated sulfuric acid as a planetary solvent could be wide-spread on exoplanets (Ballesteros et al., 2019), either on exo-Venuses or on other rocky planets that are desiccated as a result of the stellar activity of their host star (Ostberg et al., 2023). Concentrated sulfuric acid is also present in our immediate planetary vicinity, as a dominant liquid in the clouds of Venus (Titov et al., 2018), further emphasizing its importance for planetary science, planetary habitability, and astrobiology.

Our results suggest that the membranous structures observed in concentrated sulfuric acid are resistant to sulfuric acid degradation, and in some cases are dynamic. Some of the tested lipids, i.e. decylphosphonate, exhibited significantly larger aggregate sizes compared to all other samples, suggesting that the properties of a membrane could be tuned in sulfuric acid by changing the membrane lipid composition. This

observation has implications for the potential biological plausibility of such membranes, as it is analogous to the characteristics of biological membranes in water.

The confocal microscopy shows the formation of vesicles and other structures in solution but also suggests that once formed, the lipid membranes adopt a variety of morphologies and can undergo significant structural changes, such as elongation up to tens of microns in length, often with associated pearling along the elongated segment. The pearling behavior is especially noteworthy as it could facilitate division of membranous structures. Our results show that such division could in principle happen in concentrated sulfuric acid and that this solvent is compatible with complex and dynamic membranous systems.

Our experimental results are also in agreement with the QM/MM simulations. The simulations show that in the SDS-DTMA lipid membrane system the formation of a robust network of charge-charge interactions between both the head groups themselves and the solvent efficiently prevent the sulfuric acid solvent from passing through the SDS-DTMA membrane. This result raises the possibility that the SDS-DTMA membrane (or other similar lipid systems) could be robust enough to retain an aqueous vesicle lumen, or at least a distinct internal solvent environment, while keeping sulfuric acid solvent molecules from penetrating the membrane. Such membrane characteristics could in principle allow for protection and retention of acid-labile components, such as DNA, RNA, or proteins, within the vesicle.

By demonstrating the stability of lipid membranes in this aggressive solvent, we have taken a significant step forward in exploring the potential habitability of the concentrated sulfuric acid cloud environment on Venus. Future work should consider the experimental verification of the QM/MM simulations, as well as the laboratory testing of the leakage of lipid membranes resistant to concentrated sulfuric acid.

using HPC resources on the Midway3 supercomputer at the Research Computing Center at the University of Chicago.

REFERENCES
Albright LF, Houle L, Sumutka AM, et al. Alkylation of Isobutane with Butenes: Effect of Sulfuric Acid Compositions. Ind Eng Chem Process Des Dev 1972;11(3):446–450.

Apel CL, Deamer DW and Mautner MN. Self-Assembled Vesicles of Monocarboxylic Acids and Alcohols: Conditions for Stability and for the Encapsulation of Biopolymers. Biochim Biophys Acta (BBA)-Biomembranes 2002;1559(1):1–9.

Bains W, Petkowski JJ, Rimmer PB, et al. Production of Ammonia Makes Venusian Clouds Habitable and Explains Observed Cloud-Level Chemical Anomalies. Proc Natl Acad Sci 2021a;118(52).

Bains W, Petkowski JJ, Rimmer PB, et al. Production of Ammonia Makes Venusian Clouds Habitable and Explains Observed Cloud-Level Chemical Anomalies. Proc Natl Acad Sci 2021b;118(52):e2110889118.

Bains W, Petkowski JJ and Seager S. Venus' Atmospheric Chemistry and Cloud Characteristics Are Compatible with Venusian Life. Astrobiology 2023;23(10); doi: 10.1089/ast.2022.0113.

Bains W, Petkowski JJ and Seager S. Alternative Solvents for Life: Framework for Evaluation, Current Status and Future Research. arXiv Prepr arXiv240107296 2024.

Ballesteros FJ, Fernandez-Soto A and Martínez VJ. Diving into Exoplanets: Are Water Seas the Most Common? Astrobiology 2019;19(5):642–654; doi: 10.1089/ast.2017.1720.

Beyer KD, Ravishankara AR and Lovejoy ER. Measurements of UV Refractive Indices and Densities of H2SO4/H2O and H2SO4/HNO3/H2O Solutions. J Geophys Res Atmos 1996;101(D9):14519–14524.

Caschera F, de la Serna JB, Loffler PMG, et al. Stable Vesicles Composed of Monocarboxylic or Dicarboxylic Fatty Acids and Trimethylammonium Amphiphiles. Langmuir 2011;27(23):14078–14090.

Christiansen JL. Five Thousand Exoplanets at the NASA Exoplanet Archive. Nat Astron 2022;6(5):516–519.

Deamer D. Membranes and the Origin of Life: A Century of Conjecture. J Mol Evol 2016;83(5):159–168.

Gardner JP, Mather JC, Clampin M, et al. The James Webb Space Telescope. Space Sci Rev 2006;123(4):485–606; doi: 10.1007/s11214-006-8315-7.

Gebicki JM and Hicks M. Ufasomes Are Stable Particles Surrounded by Unsaturated Fatty Acid Membranes. Nature 1973;243(5404):232–234.

Griffin JM, Atherton JH and Page MI. Micelle Formation in Liquid Ammonia. J Org Chem 2015;80(14):7033–7039.

Grinspoon DH and Bullock MA. Astrobiology and Venus Exploration. Geophys Monogr Geophys Union 2007;176:191.

Habeeb A. The Reaction of Sulphuric Acid with Lysozyme and Horse Globin. Can J Biochem Physiol 1961;39(1):31–43.

Hallsworth JE, Koop T, Dallas TD, et al. Water Activity in Venus's Uninhabitable Clouds and Other Planetary Atmospheres. Nat Astron 2021;5(7):665–675.

Hargreaves WR and Deamer DW. Liposomes from Ionic, Single-Chain Amphiphiles. Biochemistry 1978;17(18):3759–3768.

Huang J and Mackerell AD. CHARMM36 All-Atom Additive Protein Force Field: Validation Based on Comparison to NMR Data. J Comput Chem 2013;34(25):2135–2145; doi: 10.1002/jcc.23354.

Humphrey W, Dalke A and Schulten K. VMD: Visual Molecular Dynamics. J Mol Graph

1996;14(1):33–38; doi: 10.1016/0263-7855(96)00018-5.

Jo S, Kim T, Iyer VG, et al. CHARMM-GUI: A Web-Based Graphical User Interface for CHARMM. J Comput Chem 2008;29(11):1859–1865; doi: 10.1002/JCC.20945.

Kanicky JR and Shah DO. Effect of Premicellar Aggregation on the p K a of Fatty Acid Soap Solutions. Langmuir 2003;19(6):2034–2038.

Kotsyurbenko OR, Cordova JA, Belov AA, et al. Exobiology of the Venusian Clouds: New Insights into Habitability through Terrestrial Models and Methods of Detection. Astrobiology 2021.

Kotsyurbenko OR, Kompanichenko VN, Brouchkov A V, et al. Different Scenarios for the Origin and the Subsequent Succession of a Hypothetical Microbial Community in the Cloud Layer of Venus. Astrobiology 2024;24(4):423–441.

Liler M. Reaction Mechanisms in Sulphuric Acid and Other Strong Acid Solutions. Academic Press: London; 1971.

Limaye SS, Mogul R, Smith DJ, et al. Venus' Spectral Signatures and the Potential for Life in the Clouds. Astrobiology 2018;18(9):1181–1198.

Liu B, Gao M, Li H, et al. Model of Protocell Compartments–Dodecyl Hydrogen Sulfate Vesicles. Phys Chem Chem Phys 2018;20(3):1332–1336.

Mansy SS. Model Protocells from Single-Chain Lipids. Int J Mol Sci 2009;10(3):835–843.

McCulloch L. Black "Soap" Films of Fatty Acids in Sulfuric Acid. J Am Chem Soc 1946;68(12):2735–2736.

Melo MCR, Bernardi RC, Rudack T, et al. NAMD Goes Quantum: An Integrative Suite for QM/MM Simulations. Nat Methods 2018;15(5):351; doi: 10.1038/NMETH.4638.

Menger FM and Jerkunica JM. Aggregation in Strong Acid. A Micelle of Carbonium Ions. J Am Chem Soc 1979;101(7):1896–1898.

Miron S and Lee RJ. Molecular Structure of Conjunct Polymers. J Chem Eng Data 1963;8(1):150–160.

Mogul R, Limaye SS, Lee YJ, et al. Potential for Phototrophy in Venus' Clouds. Astrobiology 2021a;21(10):1237–1249; doi: 10.1089/ast.2021.0032.

Mogul R, Limaye SS, Way MJ, et al. Venus' Mass Spectra Show Signs of Disequilibria in the Middle Clouds. Geophys Res Lett 2021b;e2020GL091327.

Morowitz H and Sagan C. Life in the Clouds of Venus? Nature 1967;215(5107):1259–1260; doi: 10.1038/2151259a0.

Müller A. The Behaviour of Surfactants in Concentrated Acids Part II. Formation of Micelles from Cationic Surfactants in Concentrated Sulphuric Acid. Colloids and surfaces 1991a;57(2):219–226.

Müller A. The Behaviour of Surfactants in Concentrated Acids Part III. Surface Activity of Cationics in Concentrated Sulphuric Acid. Colloids and surfaces 1991b;57(2):227–238.

Müller A. The Behaviour of Surfactants in Concentrated Acids Part IV. Investigation of the Synergism of Binary Cationic/Cationic Mixtures in Concentrated Sulphuric Acid. Colloids and surfaces 1991c;57(2):239–247.

Müller A and Burchard W. Structure Formation of Surfactants in Concentrated Sulphuric Acid: A Light Scattering Study. Colloid Polym Sci 1995;273:866–875.

Müller A and Giersberg S. The Behaviour of Surfactants in Concentrated Acids 5. Micellization and Interfacial Activity of n-Alkyltrimethylammonium Bromides in Methane Sulphonic Acid and Concentrated Sulphuric Acid. Colloids and surfaces 1991;60:309–324.

Müller A and Giersberg S. The Behaviour of Surfactants in Concentrated Acids 6. Micellization and Interfacial Behaviour of n-Hexadecyltrimethylammonium Bromide in Mixtures of Methane Sulphonic Acid and Concentrated Sulphuric Acid. Colloids and surfaces 1992;69(1):5–14.

Müller A and Miethchen R. Amphiphile Aggregation in Konzentrierten Säuren Grenzflächenaktivität von N-(N-Alkyl)-pyridinium-Salzen in Schwefelsäure. J für Prakt Chemie 1988;330(6):993–1005.

Neese F, Wennmohs F, Becker U, et al. The ORCA Quantum Chemistry Program Package. J Chem Phys 2020;152(22):224108; doi: 10.1063/5.0004608.

Ostberg C, Kane SR, Li Z, et al. The Demographics of Terrestrial Planets in the Venus Zone. Astron J 2023;165(4):168.

Patel MR, Mason JP, Nordheim TA, et al. Constraints on a Potential Aerial Biosphere on Venus: II. Ultraviolet Radiation. Icarus 2021;114796; doi: https://doi.org/10.1016/j.icarus.2021.114796.

Petkowski JJ, Seager MD, Bains W, et al. General Instability of Dipeptides in Concentrated Sulfuric Acid as Relevant for the Venus Cloud Habitability. Sci Rep 2024a;14(1):17083.

Petkowski JJ, Seager S, Grinspoon DH, et al. Astrobiological Potential of Venus Atmosphere Chemical Anomalies and Other Unexplained Cloud Properties. Astrobiology 2024b;in press.

Phillips JC, Hardy DJ, Maia JDC, et al. Scalable Molecular Dynamics on CPU and GPU Architectures with NAMD. J Chem Phys 2020;153(4); doi: 10.1063/5.0014475.

Pohorille A and Pratt LR. Is Water the Universal Solvent for Life? Orig Life Evol Biosph 2012;42(5):405–409.

Pratt LR and Pohorille A. Theory of Hydrophobicity: Transient Cavities in Molecular Liquids. Proc Natl Acad Sci 1992;89(7):2995–2999.

Reitz HC, Ferrel RE, Fraenkel-Conrat H, et al. Action of Sulfating Agents on Proteins and Model Substances. I. Concentrated Sulfuric Acid. J Am Chem Soc 1946;68(6):1024–1031.

Rhodes FH and Barbour CB. The Viscosities of Mixtures of Sulfuric Acid and Water. Ind Eng Chem 1923;15(8):850–852.

Roth U, Paulus O and Menyes U. Surface Activity of Amphiphiles in Hydrogen Fluoride—Water Solutions. Colloid Polym Sci 1995;273:800–806.

Sagnella DE and Voth GA. Structure and Dynamics of Hydronium in the Ion Channel Gramicidin A. Biophys J 1996;70(5):2043; doi: 10.1016/S0006-3495(96)79773-4.

Schulze-Makuch D and Irwin LN. The Prospect of Alien Life in Exotic Forms on Other Worlds. Naturwissenschaften 2006;93(4):155–172.

Schumacher M and Günther H. Beiträge Zur 15N-NMR-Spektroskopie Protonierung Und Tautomerie in Purinen: Purin Und 7-und 9-Methylpurin. Chem Ber 1983;116(5):2001–2014.

Seager MD, Seager S, Bains W, et al. Stability of 20 Biogenic Amino Acids in Concentrated Sulfuric Acid: Implications for the Habitability of Venus' Clouds. Astrobiology 2024a;24(4):386–396.

Seager S, Petkowski JJ, Gao P, et al. The Venusian Lower Atmosphere Haze as a Depot for Desiccated Microbial Life: A Proposed Life Cycle for Persistence of the

Venusian Aerial Biosphere. Astrobiology 2021;21(10):1206–1223.

Seager S, Petkowski JJ, Seager MD, et al. Stability of Nucleic Acid Bases in Concentrated Sulfuric Acid: Implications for the Habitability of Venus' Clouds. Proc Natl Acad Sci 2023;120(25):e2220007120; doi: 10.1073/pnas.2220007120.

Seager S, Petkowski JJ, Seager MD, et al. Year-Long Stability of Nucleic Acid Bases in Concentrated Sulfuric Acid: Implications for the Persistence of Organic Chemistry in Venus' Clouds. Life 2024b;14:538; doi: 10.3390/life14050538.

Spacek J, Rimmer P, Owens GE, et al. Production and Reactions of Organic Molecules in Clouds of Venus. ACS Earth Sp Chem 2024;8(1):89–98; doi: 10.1021/acsearthspacechem.3c00261.

Steigman J and Shane N. Micelle Formation in Concentrated Sulfuric Acid as Solvent. J Phys Chem 1965;69(3):968–973.

Sure R and Grimme S. Corrected Small Basis Set Hartree-Fock Method for Large Systems. J Comput Chem 2013;34(19):1672–1685; doi: 10.1002/JCC.23317.

Tanford C. The Hydrophobic Effect and the Organization of Living Matter. Science (80-) 1978;200(4345):1012–1018.

Titov D V, Ignatiev NI, McGouldrick K, et al. Clouds and Hazes of Venus. Space Sci Rev 2018;214(8):1–61.

Torn RD and Nathanson GM. Surface Tensions and Surface Segregation of N-Butanol in Sulfuric Acid. J Phys Chem B 2002;106(33):8064–8069.

Vanommeslaeghe K and MacKerell AD. Automation of the CHARMM General Force Field (CGenFF) I: Bond Perception and Atom Typing. J Chem Inf Model 2012;52(12):3144–3154; doi: 10.1021/CI300363C/SUPPL_FILE/CI300363C_SI_001.ZIP.

Wagner R and von Philipsborn W. Protonierung von Purin, Adenin Und Guanin NMR.-Spektren Und Strukturen Der Mono-, Di-und Tri-Kationen. Helv Chim Acta 1971;54(6):1543–1558.

Walde P, Wessicken M, Rädler U, et al. Preparation and Characterization of Vesicles from Mono-n-Alkyl Phosphates and Phosphonates. J Phys Chem B 1997;101(38):7390–7397.

Willcott MR. MestRe Nova. J Am Chem Soc 2009;131(36):13180; doi:

10.1021/ja906709t.

Zhu TF and Szostak JW. Coupled Growth and Division of Model Protocell Membranes. J Am Chem Soc 2009;131(15):5705–5713; doi: 10.1021/ja900919c.

Supplementary Information

Simple lipids form stable higher-order structures in concentrated sulfuric acid

Daniel Duzdevich[1,2,†*], Collin Nisler[1,†], Janusz J. Petkowski[3,4,5], William Bains[3,6], Caroline K. Kaminsky[1], Jack W. Szostak[1,7], Sara Seager[3,8,9]

[1] Department of Chemistry, The University of Chicago, Searle Chemistry Laboratory, Chicago, IL 60637, USA
[2] Freiburg Institute for Advanced Studies, Albert-Ludwigs-Universität Freiburg, 79104 Freiburg im Breisgau, Germany
[3] Department of Earth, Atmospheric and Planetary Sciences, Massachusetts Institute of Technology, 77 Massachusetts Avenue, Cambridge, MA 02139, USA
[4] Faculty of Environmental Engineering, Wroclaw University of Science and Technology, 50-370 Wroclaw, Poland
[5] JJ Scientific, Mazowieckie, Warsaw, Poland
[6] School of Physics and Astronomy, Cardiff University, 4 The Parade, Cardiff CF24 3AA, UK
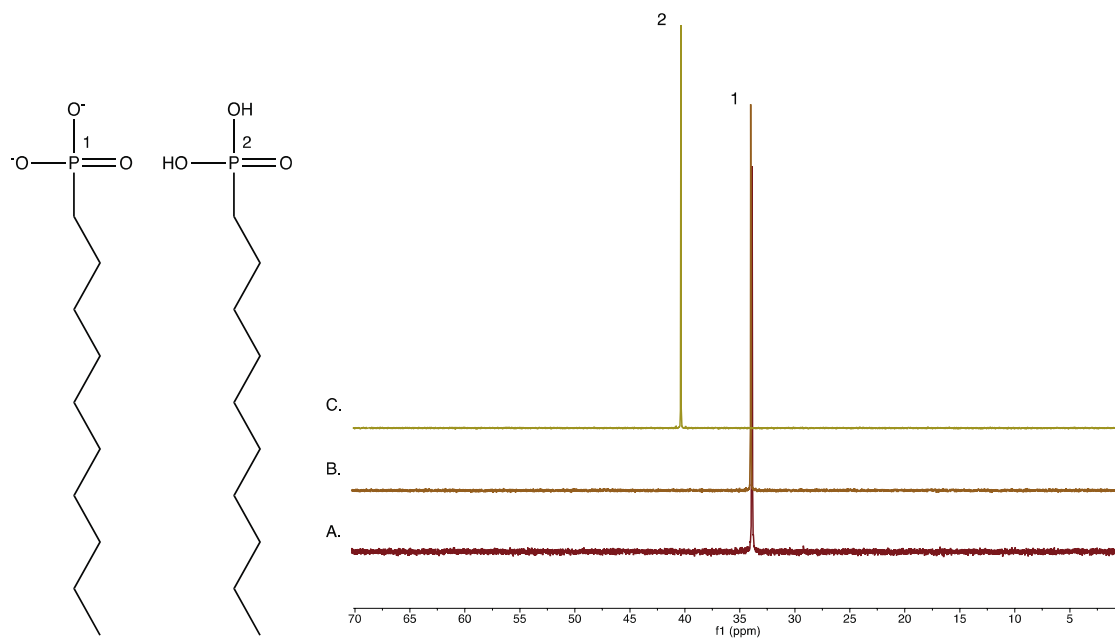[7] Howard Hughes Medical Institute, The University of Chicago, Chicago, IL 60637, United States of America
[8] Department of Physics, Massachusetts Institute of Technology, 77 Massachusetts Avenue, Cambridge, MA 02139, USA
[9] Department of Aeronautics and Astronautics, Massachusetts Institute of Technology, 77 Massachusetts Avenue, Cambridge, MA 02139, USA

[†] Equal contribution
[*] To whom correspondence should be addressed. Email: dduzdevich@uchicago.edu

Supplemental Figure 1. Decylphosphonic acid is resistant to 70% (v/v) sulfuric acid. ^{31}P NMR spectra of 50 mM decylphosphonic acid incubated in (A) D_2O, (B) D_2O + 1% H_2SO_4, and (C) 30% D_2O + 70% H_2SO_4 for one hour and extracted into $CDCl_3$. Note the absence of new peaks.
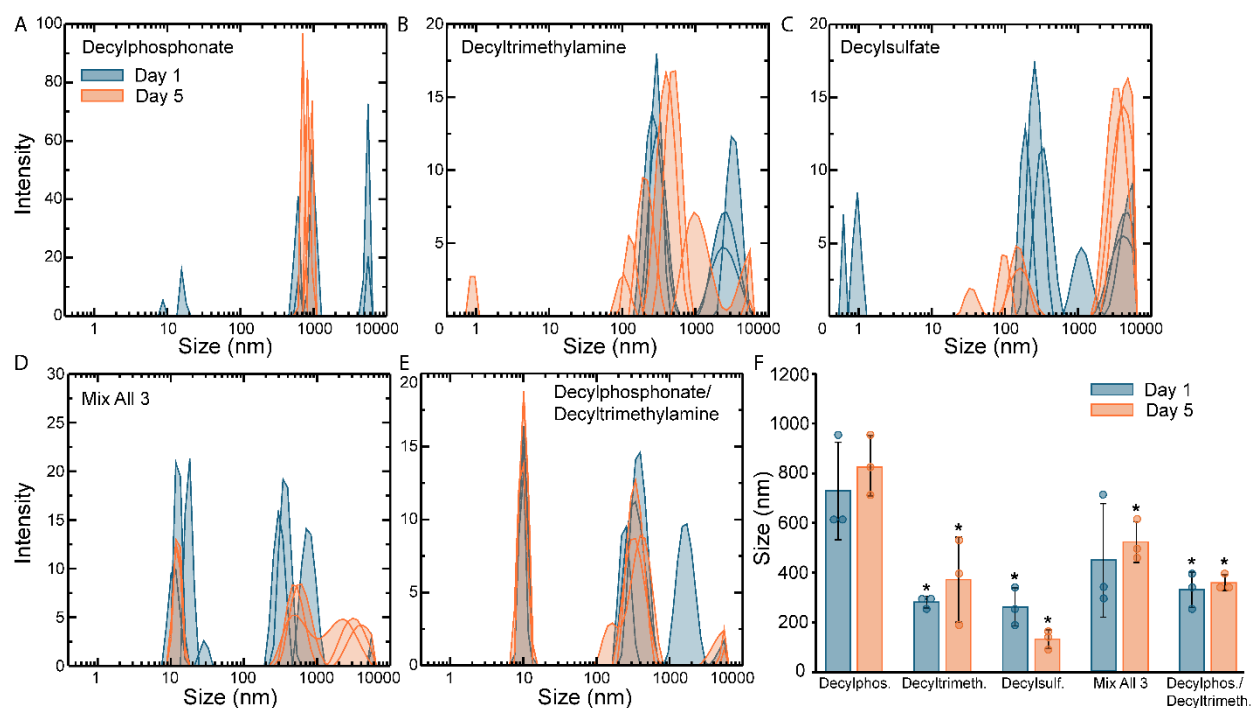
Supplemental Figure 2. Initial DLS experiments for all 3 lipids. (A-E) DLS readings of the indicated 25 mM lipids prepared in 70% sulfuric acid are shown at 24 hours (day 1) and at 5 days after preparation. All three measurements are shown for day 1 (blue) and day 5 (orange). (F) Average size of lipid structures for each lipid preparation are shown by the solid bar, individual values are indicated by circles, and standard deviations are shown in black. Sizes at peak intensity were taken for signals between 100 and 1000 nm, per analogy with 100-1000 nm vesicles sizes formed by fatty acids in water. Averages of the 3 measurements for each sample are shown by the bars, and each individual measurement value is shown in circles. Uncertainties are shown in black bars. Values that are significantly different from decylphosonate are shown by asterisks, which were the only values that exhibited significant differences between all samples. These experiments indicate that all 3 lipids can form lipid-based structures in concentrated sulfuric acid.
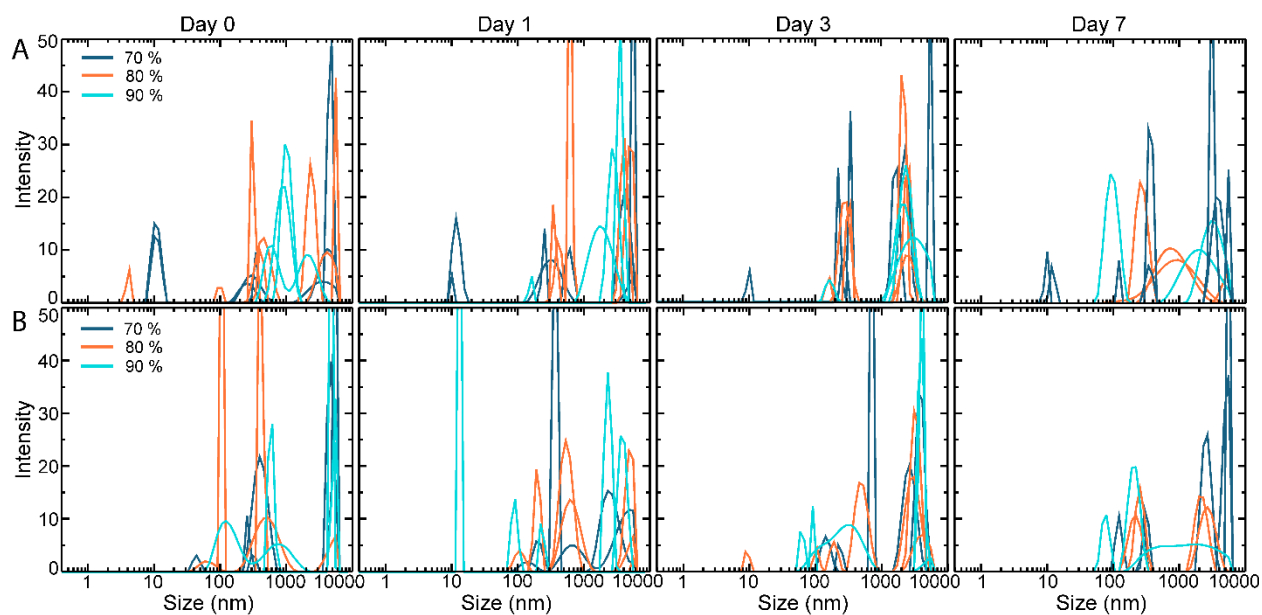
Supplemental Figure 3. All DLS experiments for all DTMA-SDS and SOS-TMO lipids. (A) DLS readings for DTMA-SDS in 70 %, 80 %, and 90 % sulfuric acid at day 0, day 1, day 3, and day 7 shown in triplicate. (B) DLS readings for SOS-TMO in 70 %, 80 %, and 90 % sulfuric acid at day 0, day 1, day 3, and day 7 shown in triplicate. While there is a significant variability observed between and among samples, such variability is supported by the microscopy results that also demonstrates a heterogeneous mix of lipid structures.
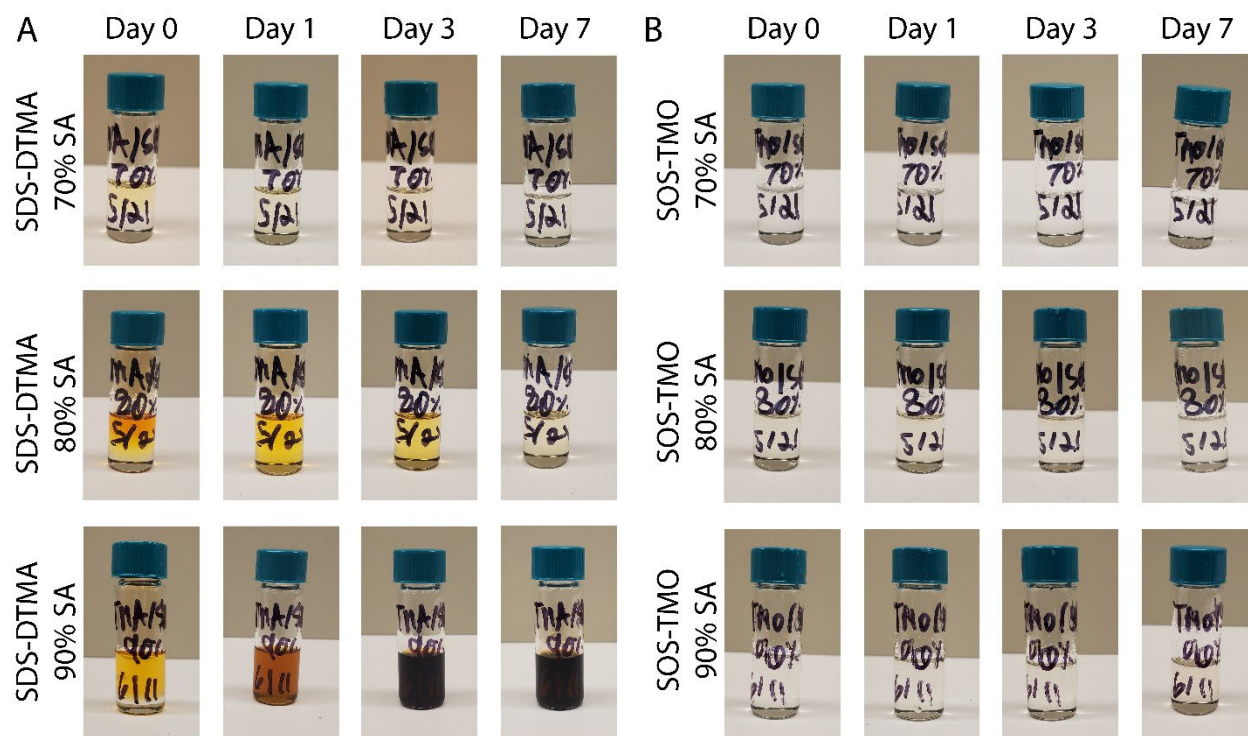
Supplemental Figure 4. Qualitative analysis of sample turbidity over time. Visual representation of the reaction between lipids and sulfuric acid for DTMA-SDS (A) and SOS-TMO (B) over the course of 7 days. DTMA-SDS lipids are reactive at concentrations above 70% acid while the SOS-TMO lipids appear stable for up to 7 days. Note that TMA-SDS in 70-80% acid seems to be getting clearer with time, with a distinct chemistry at the surface of liquid. This reactivity does not affect the formation of the lipid structures.
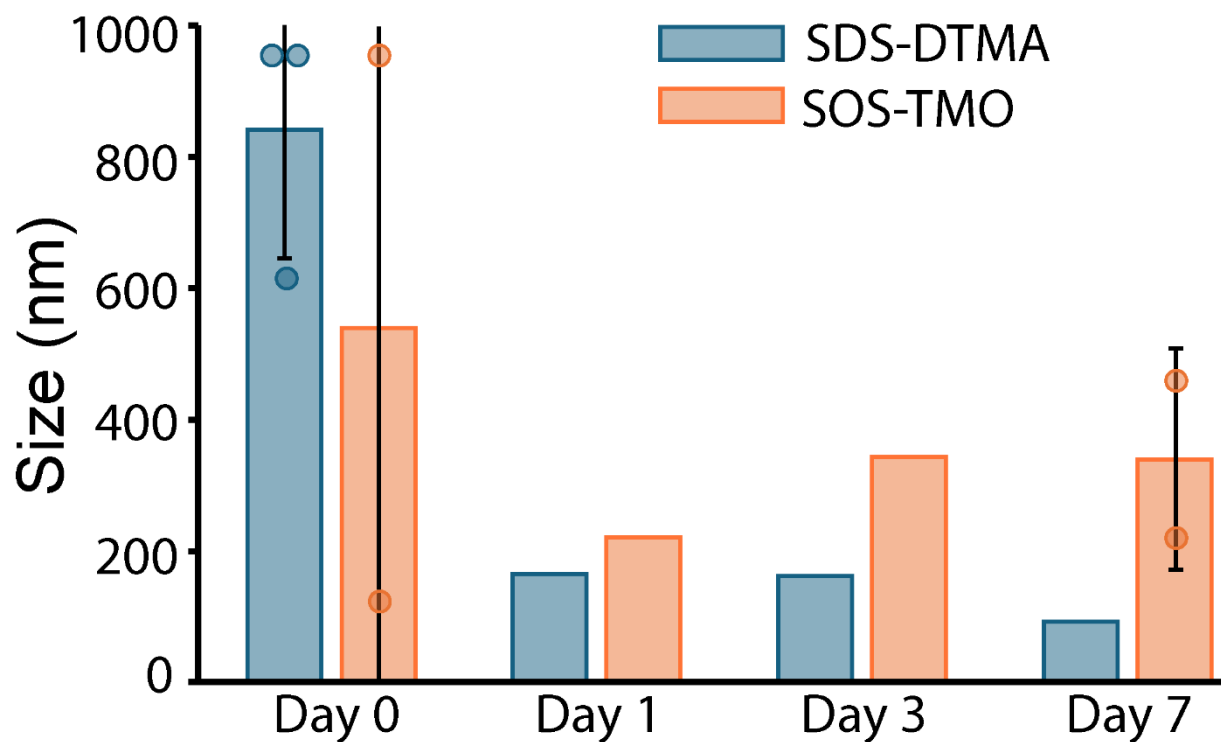
Supplemental Figure 5. Lipids form structures in 90% sulfuric acid. DLS readings of 75 mM SDS-DTMA (blue) and 1 mM SOS-TMO (orange) lipids prepared in 90% sulfuric acid are shown hours after preparation (day 0), at day 1, day 3, and day 7. While signals were observed between 100 and 1000 nm in only one replicate at day 1, day3, and SDS-DTMA day 7, shown here, the signals observed indicate that lipid-based structures are possible in 90% sulfuric acid.
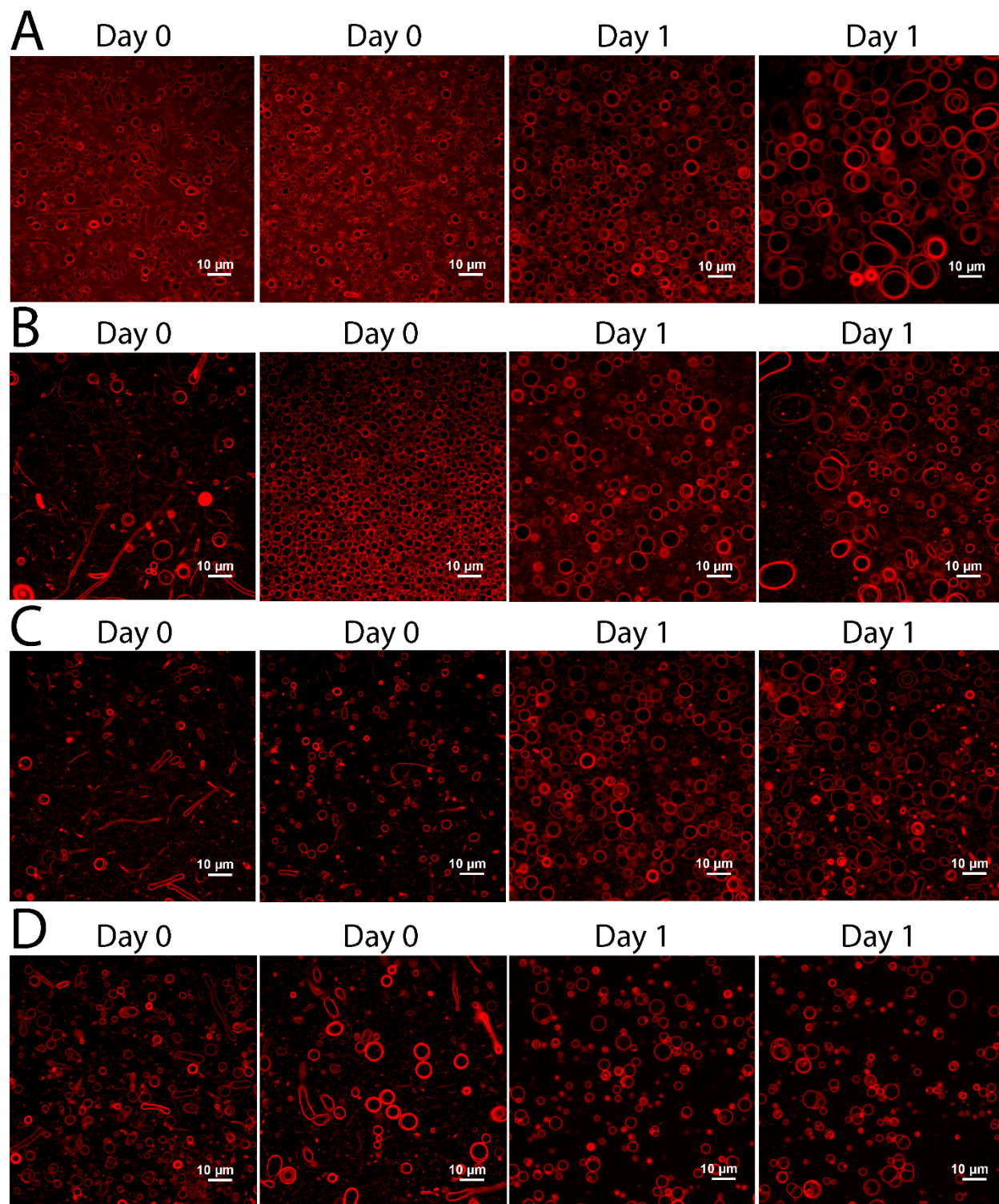
Supplemental Figure 6. SDS-DTMA vesicles are unaffected by heat shock and osmotic shock.
Confocal images of BODIPY stained SDS-DTMA lipids at day 0 and day 1 after a 65˚C heat shock (A), or after addition of water where the total final sample volume is 70% (B), 80% (C), and 90% (D) newly added water. The lack of significant morphology changes in A-D indicate those changes observed upon the addition of sulfuric acid is likely due to the change in solvent properties and not due to released heat or osmotic shock.
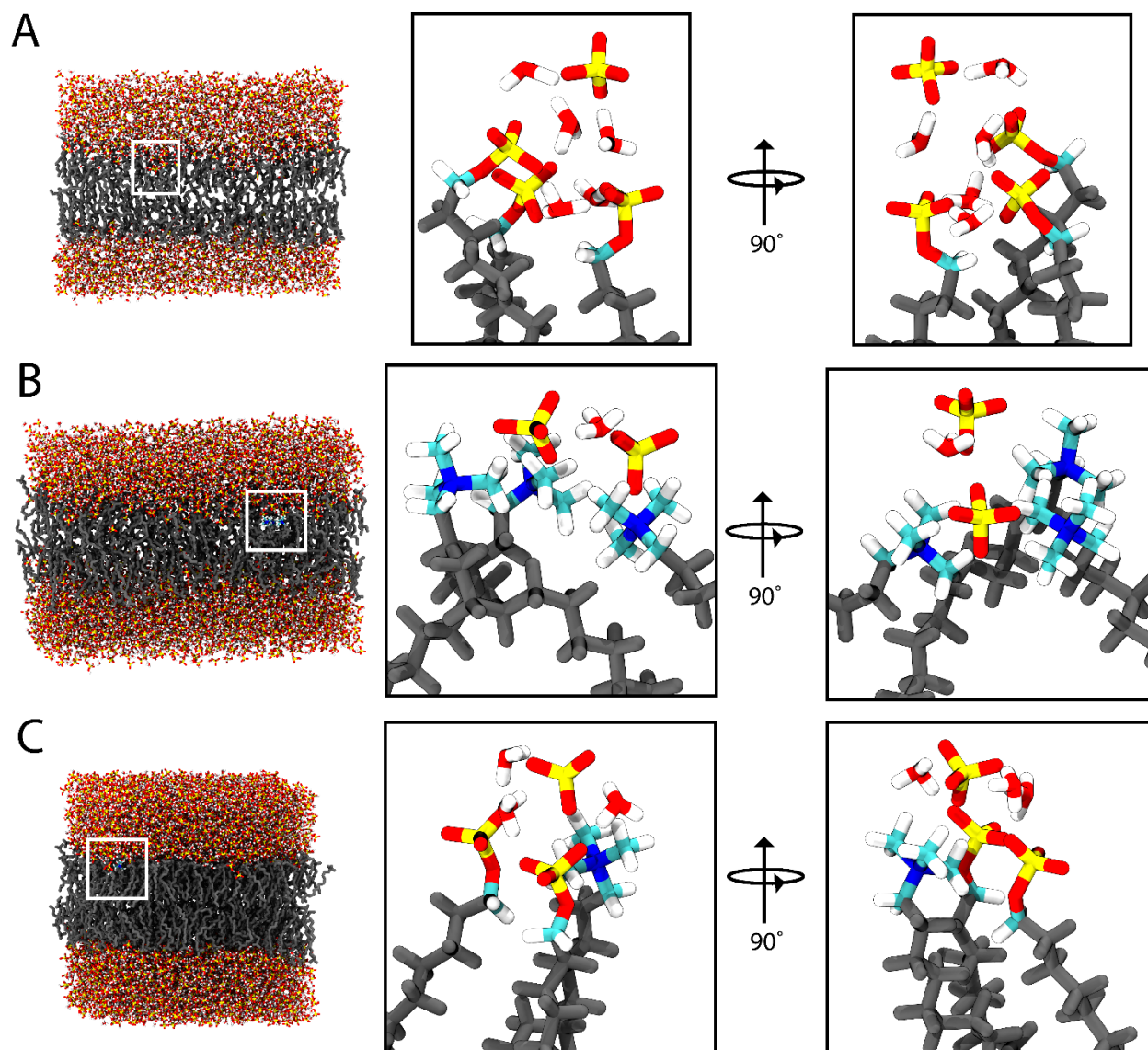
Supplemental Figure 7. Overview of simulation systems. Simulation systems Sys1a (A), Sys2a (B), and Sys3a (C). Left panels show lipids in grey and all solvent molecules explicitly, cut along the *z*-axis (perpendicular to membrane surface) at the point of the QM region. Center panels show the QM region for each system in color with the MM part of the lipid in grey, right panels show the view in the center panels rotated by 90˚.